Field Trial of High-Resolution Distributed Fiber Sensing over Multicore Fiber in Metropolitan Area with Construction Work Detection using Advanced MIMO-DAS

Sterenn Guerrier[(1)], Antonio Mecozzi[(2)], Christian Dorize[(1)], Cristian Antonelli[(2)], Lauren Dallachiesa[(3)], Haïk Mardoyan[(1)], Élie Awwad[(4)], Daniele Orsuti[(5)], Luca Palmieri[(5)], Mikael Mazur[(3)], Tetsuya Hayashi[(6)], Roland Ryf[(3)], and Jérémie Renaudier[(1)]

(1) Nokia Bell Labs, Route de Villejust, 91620 Nozay, France (2) Department of Physical and Chemical Sciences, University of L'Aquila, 67100 L'Aquila, Italy (3) Nokia Bell Labs, 600 Mountain Ave., Murray Hill, NJ 07974, USA (4) LTCI, Télécom Paris, Institut Polytechnique de Paris, 91120 Palaiseau, France (5) Department of Information Engineering, University of Padova, 35131 Padova, Italy (6) Sumitomo Electric Industries, Ltd., 1, Taya-cho, Sakae-ku, Yokohama, Kanagawa, 244-8588, Japan
sterenn.guerrier@nokia-bell-labs.com

Abstract: We demonstrate a successful field trial of MIMO-DAS over multicore fiber (MCF) allowing for accurate localization of acoustic events in the city of L'Aquila, Italy. We show a 2m spatial resolution and 1mHz-380Hz acoustic bandwidth. © 2023 The Author(s)

1. Introduction

The global fiber-optic network is both a critical communication infrastructure that needs to be constantly monitored and potentially a globally distributed sensor. Research on telecom fiber sensing is developing fast and diversely, from geophysical purposes to network telemetry [1,2]. Automated network telemetry will really thrive when the multiple sensing techniques in telecom network will be integrated with each other [3], from fiber span environment to packet loss monitoring. In that context, Distributed Acoustic Sensing (DAS) comes as the lowest granularity sensing, as it demonstrated precise localization performance over deployed single mode fiber cables [4,5]. Yet, we are approaching the limits of single-mode fiber systems: the scaling of future optical systems will require space-division multiplexing (SDM) to cope with the ceaseless increase of data traffic. Among the SDM approaches, the use of multi-core fibers (MCFs) is gaining momentum. Recently, real-time transmissions over 4-coupled-core MCFs have been demonstrated either in lab experiment [6], or in a field trial [7]. In the latter, the MCF cable was deployed in a tunnel beneath the city of L'Aquila, Italy [8]. Beyond the transmission results, the transmitted state of polarization over the deployed cable was analyzed as very stable in time [7], although no distributed sensing experiment was conducted yet. In this paper, we demonstrate for the first time the operability of advanced DAS [9] over MCF and show distributed measurements with down to 2 m spatial resolution. We extract phase and polarization from the backscattered Jones matrices for reliable retrieval of the acoustic events in the city, successfully localizing and identifying construction works-related events.

2. Experimental Setup

The experimental set-up is displayed in Fig. 1(a). The laser source feeds the coherent multiple-input multiple-output (MIMO-) DAS system. After modulation, the signal is connected to core 1 of a 4-core uncoupled-core MCF (UC-

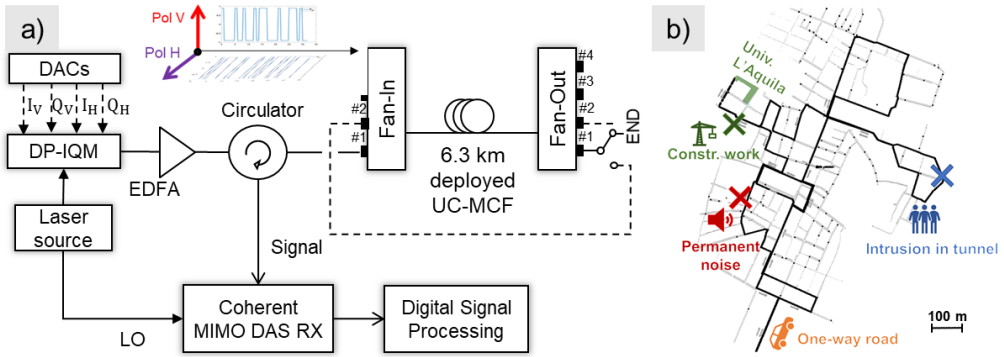

Fig. 1: Experimental set-up. (a) Coherent-MIMO DAS interrogator and MCF connection set-up. DP-IQM: Dual-pol. I/Q modulator ; DACs: Digital-to-Analog Converters (b) Map of the 6.3-km MCF testbed in L'Aquila, markers for set of events (construction works, permanent noise, road traffic, and intentionally produced perturbations in the tunnel)

MCF) through the Fan-In-Fan-Out (FIFO), yielding a 6.3 km sensing path. Looping the output of core 1 back to the input of core 2 yields a 12.6-km overall sensing path, going through 1 or 2 loops under the city of L'Aquila along the path displayed in Fig. 1(b). The MCF is deployed in the top-right shelves of a multiservice tunnel under the city at about 2 m below the ground. Note that the first 304 m and last 355 m of the MCF are stacked in the lab and therefore not exposed to the potential disturbances in the tunnel, rather to the air conditioning (AC) unit in the lab. The Coherent-MIMO-DAS transmits dual-polarization signals modulated with bipolar coded sequences (or "codes") [10] at a symbol rate of 50 MBaud with code repetition rate T_{code}=1.3 ms. The backscattered light is passed through an optical circulator and sent to a dual-polarization coherent receiver, then sampled at a rate of f_{samp}=100 MS/s yielding a theoretical spatial resolution of S_r=1.02 m [11].

3. Field trial map results

From a 20-minute interrogation of the two cores, we first extract a map of the differential backscattered phase variations σ_ϕ in the time-distance plane: the standard deviation of phase in time is computed in Fig. 2 for every segment of the fiber, with brighter points corresponding to stronger variations (dark for silent zones). The phase variations are mapped in logscale. The markers on top of the figure relate to the events illustrated in Fig. 1(b). Even though the tunnel appears as rather silent [7], the backscattered phase variations do catch various events along the fiber path. In addition to the vertical lines which are motionless disturbances, one can notice mirrored portions of the map: [1.8–2.2] km and [2.6–3] km which correspond to a section of cable installed along a roundtrip path below a road, yielding symmetric oblique waterfall traces (red square in Fig. 2(a), car icon in Fig. 1(b)).

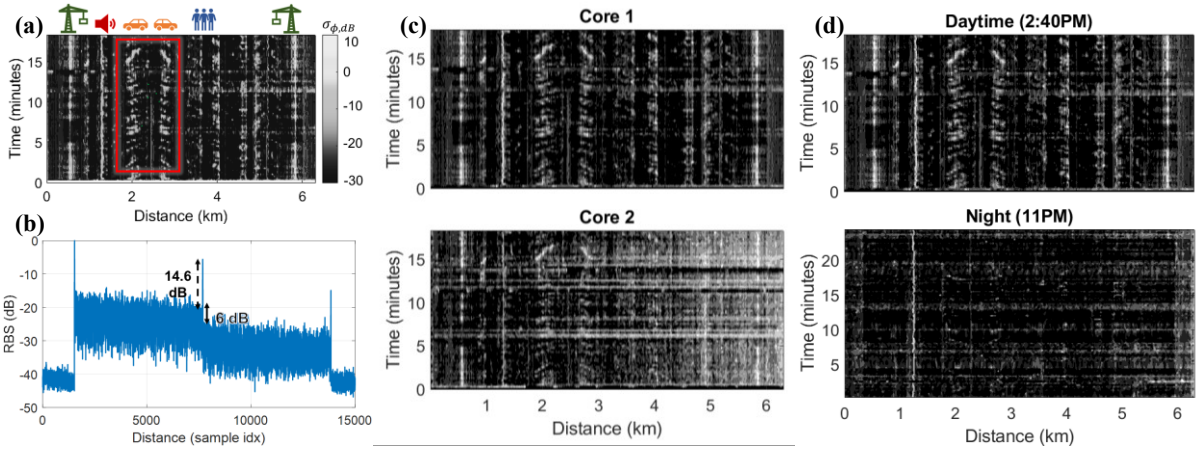

Fig. 2: (a) Time-Distance map of phase variations on one core of deployed fiber, top markers for set of identified events & red square for traffic-related oblique traces. (b) Backscattered intensity and reflection at the interface of two-core set-up (c) compared time-distance map for the successive cores (d) Daytime (2:50PM) map of core 1 compared to night (11PM) map.

To cross-validate the observed results, we cascade two cores of the same MCF. However, the pass through the FIFO yields both reflections and connection losses, as displayed in Fig. 2(b), hence a lowered backscattered power from core 2, leading to lower reliability (lighter zones in Fig. 2(c)) [12]. The two cores have independent Rayleigh scatterers distributions, yet they are exposed to the same acoustic events and a good match is observed between cores in Fig. 2(c): the accuracy of event detection can be enhanced by the multi-core detection.

4. Localized events

The underground tunnel serves multiple purposes, including water and electricity supply in the city downtown area. Thus, some water pumps or electrical devices permanently operate around the tunnel, while the traffic and construction work outside start and stop according to the time of the day. In Fig. 2(d), we compare the phase variations map in core 1 during day and night and observe a continuous disturbance due to the surrounding devices around 1.2 km, while most other static events have faded. Note that during the night, the fiber sections in the lab (the first 304 m and last 355 m in Fig. 2(d)) capture more acoustic events than those in the tunnel, as the AC unit is still running. Fig. 3(a) shows the power spectral density (PSD) of the backscattered phase variations due to these surrounding devices' noise (red, main frequency peak 7.8 Hz) and of one lab segment, which is impacted by the fluctuations of the AC (gray, cross marker, main frequency peak 91.7 Hz). Identification and classification of the events can be obtained from such PSD measurements. Back to Fig. 2(a), we notice a discontinuous line of events

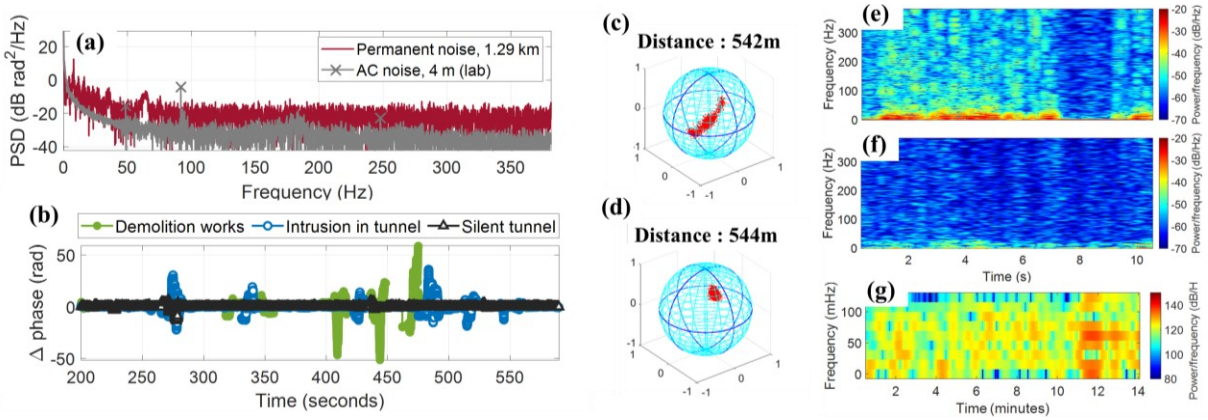

Fig. 3: (a) Backscattered phase measurements using MIMO-DAS in frequency domain and (b) time domain, (c,d) polarization rotation vector, (e,f) spectrograms of pol. averaged phase standard deviation respectively at 542 m from fiber start (impact) and 544 m (after impact), 10 s. (g) Spectrogram of downsampled pol. avg. phase std, 542 m, 15 mn.

around 530 m from the start and the end of the fiber (green crane markers). It corresponds to strong vibrational events occurring in a street 104 m away from the university lab, the start of the tunnel loop, meaning after 220 m of deployed MCF (the remaining fiber distance being coiled in the lab): a building was demolished during the trial in the street behind the university (Fig. 1(b)). Also, Fig. 3(b) shows the differential phases at 3.6 km in a silent tunnel section, at 3.8 km where people entered the tunnel, and at 0.54 km from the fiber start where a building is demolished, respectively. The phase is strongly disturbed: up to 35.8 rad and 57.8 rad phase excursions were measured for intrusion and demolition, respectively. For such strong events, it is not suitable to rely solely on the phase to identify the acoustic event, so we also look at the backscattered polarization states. Fig. 3(c,d) shows the polarization rotation vector extracted from the unitary part of the roundtrip propagation matrix and Fig. 3(e-g) the polarization averaged phase spectrograms [13,14] at the location where construction work was detected (c,e), and at the adjacent segment (d,f) in a 10-s time window. The rapid changes of the polarization rotation vector and the subsequent [0-20] Hz vibrations are clearly visible, whereas the adjacent segment shows a limited polarization evolution. Results in Fig. 3(c-f) are obtained with a gauge length (as defined in [15]) of 2 m. The vibrations also affect the higher frequencies in Fig. 3(e), as such events also yield audible acoustic frequencies (>20 Hz, measured up to 380 Hz here). Fig. 3(g) displays the downsampled spectrogram of polarization averaged phase variations at 542 m. Several events of power above 120 dB/Hz are observed down to the mHz range at low frequency resulting from the demolition works, illustrating the capability of the DAS to capture a broad spectrum of vibrational events.

5. Conclusions

We demonstrated the first successful operation of MIMO-DAS over MCF. The usage of backscattered Jones matrices allowed for a multidimensional approach of physical layer telemetry. Clear detection and localization of construction works over distinct cores of the MCF, with 2 m spatial resolution, was demonstrated, paving the way for early warning of costly hazardous events such as fiber cuts.

Acknowledgement: This work is partially supported by the Italian Government under projects INCIPICT and PRIN2017 FIRST.

References

[1] T. Wang, M. Huang et al., "Employing Fiber Sensing and On-Premise AI Solutions for Cable Safety …," in OFC 2022, paper Th3G.1.
[2] Mecozzi, et al. "Polarization Sensing Using Submarine Optical Cables." Optica 2021, 8 (6), 788. https://doi.org/10.1364/OPTICA.424307
[3] V. Vusirikala, "Optical networking long term vision: a hyperscaler perspective," in OFC 2021, invited paper, M1A.3, San Francisco, 2021.
[4] E. Ip, et al., "DAS over 1,007-km Hybrid Link with 10-Tb/s DP-16QAM Co-propagation …," in OFC 2022, paper Th4A.2.
[5] S. Guerrier, et al. "Vibration Detection and Localization in Buried Fiber Cable after 80km …" In OFC 2022, paper M2F.3.
[6] S. Beppu et al., "Real-Time Transoceanic Coupled 4-Core Fiber Transmission". In OFC 2021 https://doi.org/10.1364/OFC.2021.F3B.4
[7] M. Mazur, et al., "Real-Time MIMO Transmission over Field-Deployed Coupled-Core Multi-Core Fibers," in OFC 2022, paper Th4B.8
[8] Hayashi, T. et al., "Field-Deployed Multi-Core Fiber Testbed," OECC2019, https://doi.org/10.23919/PS.2019.8818058
[9] Guerrier, S. et al., "Introducing Coherent MIMO, a Fading-Resilient Approach to ϕ-OTDR." Opt. Exp. 2020, vol. 28, no. 14, p.21081
[10] Dorize, C.& Awwad, E. "Enhancing the Performance of Coherent OTDR Systems…". Opt. Express 2018, vol.26, no.10, 12878.
[11] Liokumovich, L. B.; et al., "Fundamentals of Optical Fiber Sensing Schemes Based on …". JLT 2015, vol. 33, no. 17, pp. 3660–3671.
[12] Dorize, C. et al., "Identification of Rayleigh Fading Induced Phase Artifacts in Coherent …". Opt. Lett. 2021, vol. 46, no. 11, p.2754.
[13] Damask, J. N. "Polarization Optics in Telecommunications"; Springer Science & Business Media, 2004; Vol. 101.
[14] A. Mecozzi, et al., "Use of optical coherent detection for environmental sensing," ECOC22, Basel, Switzerland, 2022. paper Tu3D.1
[15] SEAFOM, "DAS Parameter Definitions and Tests," http://seafom.com, measuring sensor performance-02 ed. (2018).